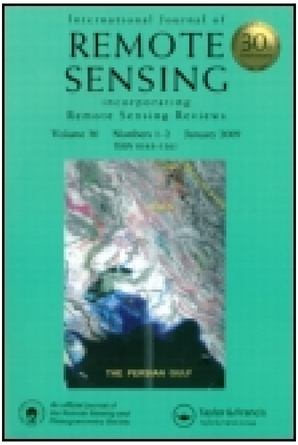

International Journal of Remote Sensing
Publication details, including instructions for authors and subscription information:
http://www.tandfonline.com/loi/tres20

Cover. Wind energy mapping of coastal zones by synthetic aperture radar (SAR) for siting potential windmill locations

O. M. Johannessen & E. Bjorgo

Available online: 25 Nov 2010

INT. J. REMOTE SENSING, 2000, VOL. 21, NO. 9, 1781–1786

Cover

Wind energy mapping of coastal zones by synthetic aperture radar (SAR) for siting potential windmill locations

O. M. JOHANNESSEN

Nansen Environmental and Remote Sensing Center, Edvard Griegsvei 3A, N-5059 Bergen, Norway

and E. BJORGO

Terra Orbit Ltd., Edvard Griegsvei 3A, N-5059 Bergen, Norway

The Earth's population is facing an increasing demand for electrical power. After the Kyoto meeting which gave clear signals of reductions in the CO_2 emission to the atmosphere it is clear that new alternative sources of power must be considered to meet those needs. In this context it has been focused on possibilities for increasing the utilization of converting wind energy into electrical power by use of wind mills. With the technical improvement of wind power turbines in recent years, operating wind power-plants have become more economically efficient, and is today a worthy source for complementing other types of energy.

In planning for wind mill park installations it is of fundamental importance to have sufficient information about the wind characteristics for different seasons. Standard wind measurements are available from ground mounted instruments, such as cup- or sonic anemometers which usually provides time series of averaged 1 or 10 minutes intervals. Such measurements are very local and will not properly resolve the spatial variations in the wind field and it is thus generally difficult to estimate wind conditions at a nearby site. Since surface wind fields have large spatial variations, mapping of the wind field with high spatial resolution is of great importance for wind mill siting.

The cover (and figure 1) illustrates the method of mapping wind energy in coastal zones for potential wind power plant location using synthetic aperture radar (SAR) derived wind speed, as suggested for the first time by Johannessen *et al.* (1998). The SAR instrument has clear advantages for high spatial resolution wind field mapping since it penetrates clouds and is not dependent on sun illumination of the remotely sensed objects. The SAR instruments onboard European Space Agency (ESA) ERS-1&2 and the Canadian RADARSAT have sufficient spatial resolution, 30 m and 10 m respectively, as well as 100 km (ERS-1&2) and 500 km (RADARSAT) wide spatial coverage along the coastline. Wind maps generated from SAR will be able to provide spatial information about sea surface wind energy at approximately 400 m

International Journal of Remote Sensing
ISSN 0143-1161 print/ISSN 1366-5901 online © 2000 Taylor & Francis Ltd
http://www.tandf.co.uk/journals

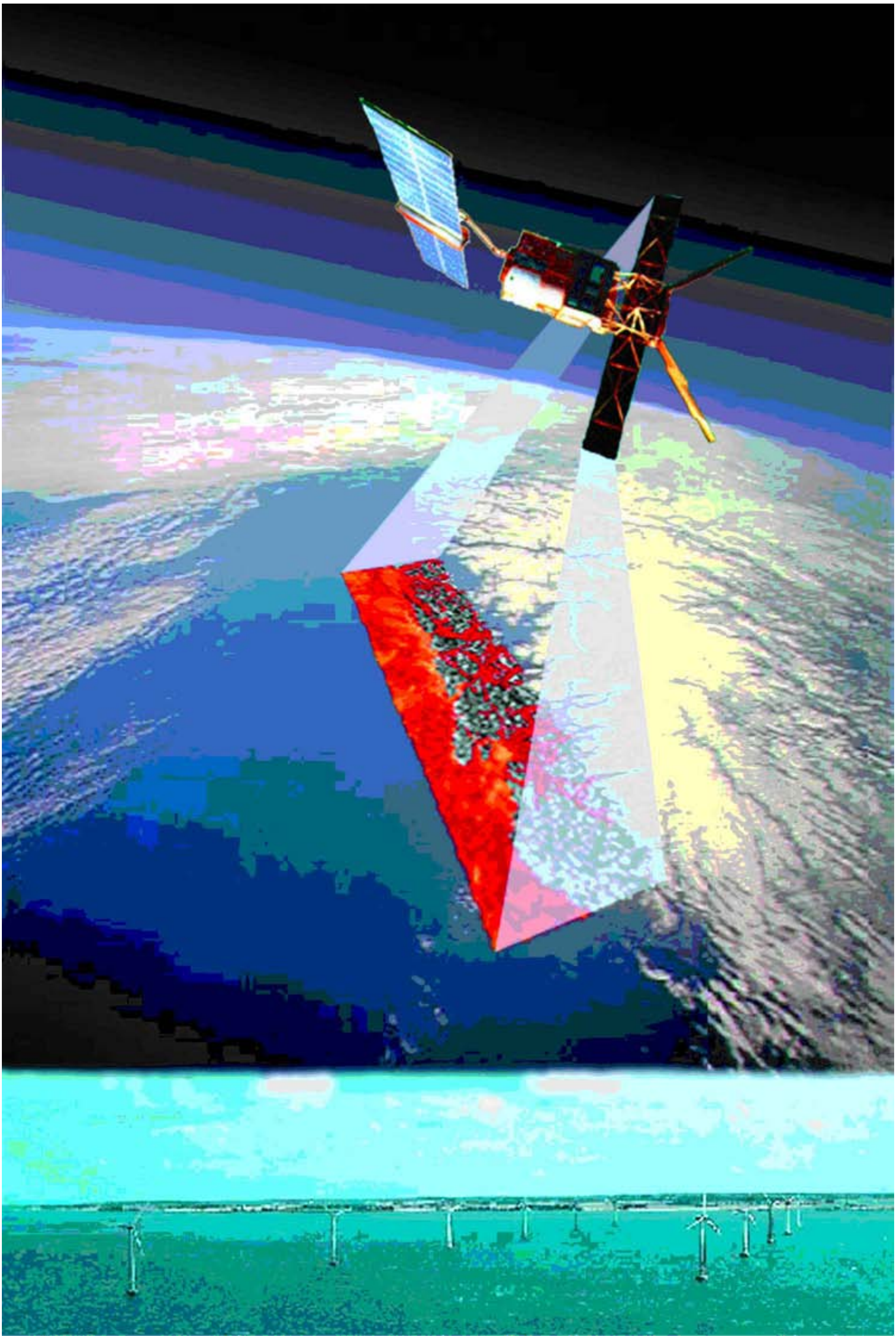

Figure 1. The method of mapping wind energy in coastal zones for potential wind power.

resolution. This information can be extrapolated using boundary layer theory to provide wind energy estimates at wind mill heights.

In SAR images, the reflected amount of energy will be proportional to a power of the surface wind speed. The radar signal is reflected by capillary waves with a scale comparable to the wavelength (~5 cm) of the signal. These waves will be created instantly with the wind speed and is therefore an indicator of the surface wind speed. During several experiments empirical relations between the wind speed (normalized to 10 m above the surface) and the received reflected radar signal from the surface have been established. These relations are known as C band models

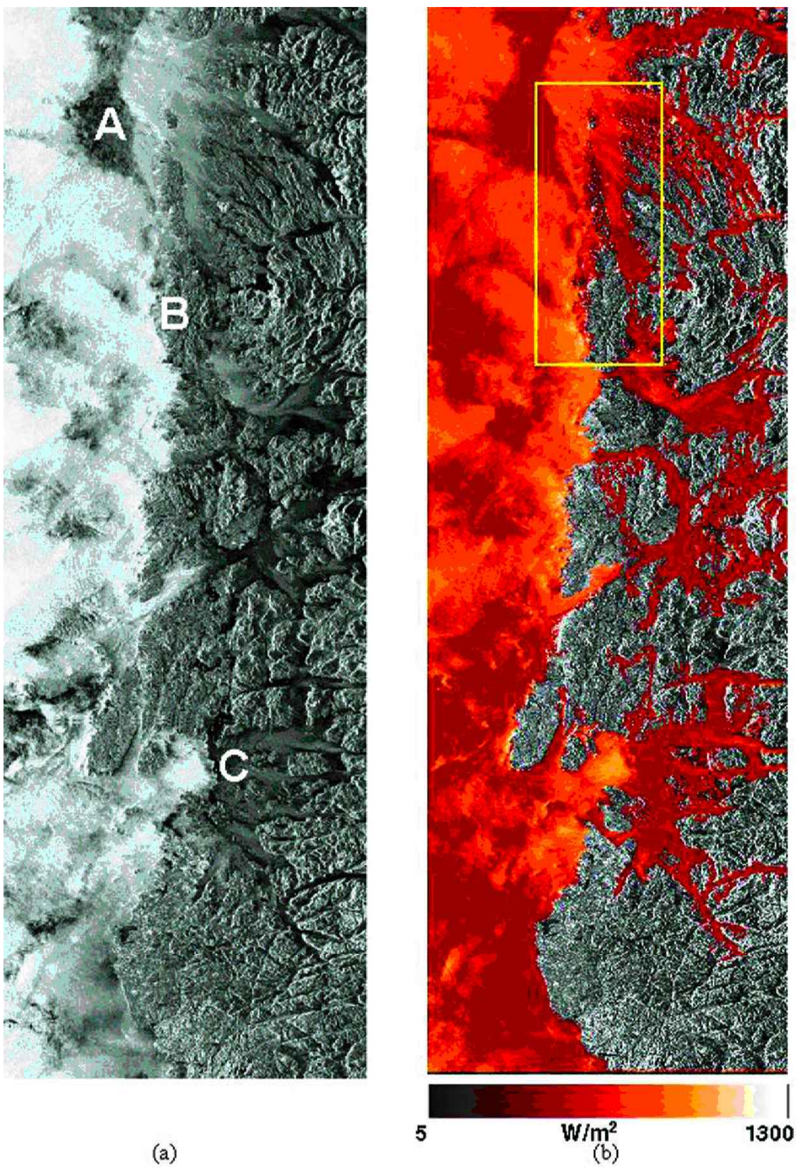

Figure 2. SAR image from Norwegian west-coast (left) and corresponding map of wind energy at 10 m height (right). Brighter areas indicate more wind energy.

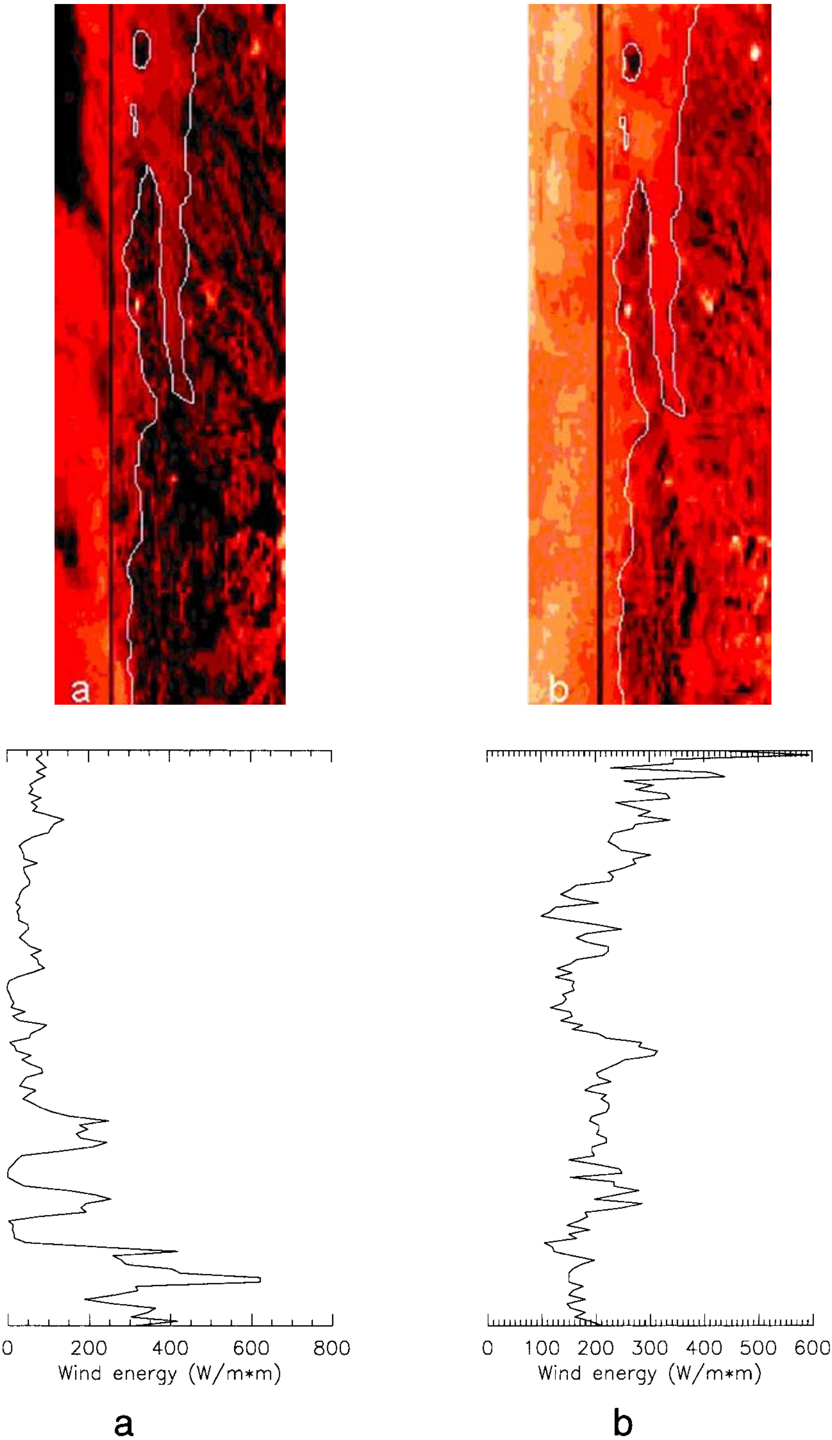

Figure 3. Wind energy maps (top) from two different ERS-1 passes and the corresponding variations in energy variation along a profile at 10 m height following the black vertical line in the two top figures. The selected area is indicated with a yellow rectangle in figure 2 (*b*).

(CMOD) and their applications and accuracy (normally within $\pm 2\,\mathrm{m\,s^{-1}}$) for SAR is reported in e.g. Vachon *et al.* (1996), Scoon *et al.* (1996), and Korsbakken *et al.* (1998). For wind energy mapping the spatial distribution of the wind speed, as derived using the CMOD algorithm (Quilfen *et al.* 1998) is turned into wind energy using the relationship $\mathrm{E} = 0.5 \times 1.225 \times v^3$, where v is the wind speed in $\mathrm{m\,s^{-1}}$, for air density of $1.225\,\mathrm{kg\,m^{-3}}$, corresponding to dry air at standard atmospheric pressure at sea level at 15°C (Johannessen and Korsbakken, 1998).

In figure 2 (*a*), three standard ERS-1 SAR precision image (PRI) scenes from the Norwegian west coast are merged to cover a 100 km by 300 km area. The SAR PRI has an initial spatial resolution of about $30\,\mathrm{m} \times 30\,\mathrm{m}$ but is block averaged to a spatial resolution of $400\,\mathrm{m} \times 400\,\mathrm{m}$ to reduce speckle noise and improve the statistical significance for wind speed in each pixel, still allowing detailed mapping of the wind energy in the coastal zone. Figure 2 (*b*) illustrates the corresponding wind energy at 10 m height. In the SAR image (figure 2 (*a*)) we have indicated dark areas with relatively low wind speed (A), bright areas with higher wind speeds close to shore (B), and a wind front in fjord area (C). The wind speeds range here from below $2\,\mathrm{m\,s^{-1}}$ to approximately $8\,\mathrm{m\,s^{-1}}$. The wind speeds were calculated using the average wind direction from a synoptic meteorological map of the area. The energy flux ($\mathrm{W\,m^{-2}}$ at 10 m height) plot in figure 2 (*b*) clearly reveals areas of low and high energy all the way into the coast and fjord areas. The energy ranges from about $5\,\mathrm{W\,m^{-2}}$ up to about $1300\,\mathrm{W\,m^{-2}}$. With an average wind speed of $4.5\,\mathrm{m\,s^{-1}}$ at hub height (50–100 m) the average wind mill will generate about 500 000 kWh per year. With an average wind speed of 9 meters per second it will generate 2 400 000 kWh per year. Thus, doubling the average wind speed has increased energy output 4.8 times. Note that this example is only a temporal 'snapshot' and does not represent wind energy distribution maps used as statistical background material in locating optimal sites for wind power plant construction. More SAR scenes are needed for producing such maps.

Figure 3 illustrates the importance of optimum siting. From the energy field a profile is extracted along the black line. Such a profile will represent the total instant energy flux ($\mathrm{W\,m^{-2}}$) at 10 m heigt. Such plots, arranged chronologically for several images, as shown in figure 3 for only two days, will reveal regional and seasonal variations in the energy distribution.

SAR wind energy maps have the potential to be used for large-and regional scale mapping in order to select areas of interest for wind power plant development world wide, and should be complementary to more detailed *in situ* measurements and mathematical modelling once potential sites have been identified in the satellite derived products.

References

Johannessen, O. M., Korsbakken, E., and Bjørgo E., 1998, Determination of wind energy from synthetic aperture radar images for wind mill siting. *Proceedings of the 27th International Symposium on Remote Sensing of Environment, Tromsø, Norway, 8–12 June 1998* (Columbia: I.S.R.S.E.), pp. 217–220.

Johannessen, O. M., and Korsbakken, E., 1998, Wind mill siting from ERS SAR. *ESA Earth Observation Quarterly*, **59**, 2–4.

Johannessen, O. M., Johannessen, J. A., Jenkins, A. D., Davidson, K., Lyzenga, D. R., Shuchman, R., Samuel, P., Espedal, H. A., Knulst, J., Dano, E., and Reistad, M., 1996, Coast Watch-95: ERS-1/2 SAR applications of mesoscale upper ocean and atmospheric boundary layer processes off the coast of Norway. *Proceedings of the*

International Geoscience and Remote Sensing Symposium, Lincoln, Nebrasca, 27-31 May 1996 (Houston: I.E.E.E.), pp. 1158–1161.

Korsbakken, E., Johannessen, J. A., and Johannessen, O. M., 1998, Coastal wind field retrievals from ERS synthetic aperture radar images. *Journal of Geophysical Research*, **103**, 7857–7874.

Quilfen, Y., Chapron, B., Elfouhaily, T., Katsaros, K., and Tournadre, J., 1998, Observation of tropical cyclones by high-resolution scatterometry. *Journal of Geophysical Research*, **103**, 7767–7786.

Scoon, A., Robinson, I. S., and Meadows, P. J., 1996, Demonstration of an improved calibration scheme for ERS-1 SAR imagery using a scatterometer wind model. *International Journal of Remote Sensing*, **17**, 413–418.

Vachon, P. W., and Dobson, F. W., 1996, Validation of wind vector retrieval from ERS-1 SAR images over the ocean. *The Global Atmosphere and Ocean System*, **5**, 177–187.